In Vitro Drug-Drug Interaction Evaluation of GalNAc Conjugated siRNAs Against CYP450 Enzymes and Transporters

Author List: Diane Ramsden, Jing-Tao Wu, Brad Zerler, Sajida Iqbal, Jim Jiang, Valerie Clausen, Krishna Aluri, Yongli Gu, Sean Dennin, Joohwan Kim and Saeho Chong

Alnylam Pharmaceuticals, Inc., Cambridge, Massachusetts (DR, JTW, JJ, VC, KA, YG, SD, JK and SC)

The Medicines Company, Parsippany, New Jersey (BZ)

Sanofi, Waltham, Massachusetts (SI)

Running title:

In vitro DDI investigations for GalNAc-siRNA

Corresponding Author:

Diane Ramsden

Drug Metabolism and Pharmacokinetics, early Development

Alnylam Pharmaceuticals

300 Third Street

Cambridge, MA 02142

Telephone: 617.575.7390

Email: dramsden@alnylam.com

Number of text pages: 27

Number of Tables: 6

Number of Figures: 4

Number of References: 34

Number of words in Abstract: 249

Number of words in Significance Statement: 105

Number of words in Introduction: 694

Number of words in Discussion: 1226

Number of Supplementary Tables: 6

Abbreviations

CYP, cytochrome P450; siRNA, small interfering ribonucleic acid; GalNAc, N-acetylgalactosamine; CL_{int}, intrinsic clearance; ESC, enhanced stabilization chemistry; STC, standard template chemistry; NADPH, β-nicotinamide adenine dinucleotide phosphate reduced form; NADH, β-nicotinamide adenine dinucleotide reduced form; ASGPR, asialoglycoprotein receptor; AUC, area under the concentration vs. time curve; AUCR, AUC ratio; CAR, constitutive androstane receptor; $C_{max,}$ maximum concentration; CRO, contract research organization: Ct, cycle time; DDI(s), drug-drug interaction(s); DME, drug metabolizing enzymes; DMSO, dimethylsulfoxide; EMA, European medicines agency; E_{max}, maximum fold increase (or induction) minus baseline of 1-fold; F2, the concentration achieving 2-fold induction; FDA, food and drug administration; fmCYP, fraction metabolized by CYP; GAPDH, glyceraldehyde 3 phosphate dehydrogenase; Ind_{max}, maximal fold induction; IVIVE, in vitro in vivo extrapolation; PMDA, pharmaceutical and medical devices agency; PK, pharmacokinetics; PXR, pregnane-X receptor; TDI, time dependent inhibition; UWDID University of Washington drug-drug interaction database

Abstract

Small interfering RNAs (siRNAs) represent a new class of medicines that are smaller (~16,000 Da) than biological therapeutics (>150,000 Da) but much larger than small molecules (<900 Da). Current regulatory guidance on drug-drug interaction (DDI) from EMA, FDA, and PMDA provide no recommendations for oligonucleotide therapeutics including siRNAs, therefore small molecule guidance documents have historically been applied. Over ~10 years, in vitro DDI investigations with siRNAs conjugated to a triantennary N-acetylgalactosamine ligand (GalNAc-siRNAs) have been conducted during nonclinical drug development to elucidate the potential clinical DDI liability. GalNAc-siRNAs were evaluated as substrates, inhibitors or inducers of major CYPs and as substrates and inhibitors of transporters. Aggregate analysis of these data demonstrates a low potential for DDI against CYPs. Zero of five, ten and seven are inducers, time-dependent inhibitors, or substrates, respectively, and 9 of 12 do not inhibit any CYP isoform evaluated. Three GalNAc-siRNAs inhibited CYP2C8 at supratherapeutic concentrations, and one mildly inhibited CYP2B6. The lowest K_i of 28 µM is >3000-fold above the therapeutic clinical $C_{max,ss}$ and importantly no clinical inhibition was projected. Of four GalNAc siRNAs tested none were substrates for transporters and one caused inhibition of P-gp, calculated not to be clinically relevant. Pharmacological basis for DDI, including consideration of the target and/or off-target profile for GalNAc-siRNAs should be made as part of the overall DDI risk assessment. If modulation of the target protein doesn't interfere with CYPs or transporters, then in vitro or clinical investigations into the DDI potential of the GalNAc-siRNAs are not warranted.

Significance Statement

Recommendations for evaluating DDI potential of small molecule drugs are well established, however guidance for novel modalities, particularly oligonucleotide-based therapeutics are lacking. Given the paucity of published data in this field in vitro DDI investigations are often conducted. The aggregate analysis of GalNAc-siRNA data reviewed herein demonstrates that like new biological entities (NBEs), these oligonucleotide-based therapeutics are unlikely to result in DDI, and therefore it is recommended that the need for in vitro or clinical investigations similarly be determined on a case-by-case basis. Given the mechanism of siRNA action, special consideration should be made in cases where there may be a pharmacological basis for DDI.

Introduction

Harnessing the endogenous gene regulatory pathway of RNA interference (RNAi) is possible using chemically modified small interfering ribonucleic acids (siRNA) that induce short term silencing of proteins and represent a new class of drugs (Kim and Rossi, 2008). When introduced into cells, the guide (or antisense) strand of the siRNA loads into an enzyme complex called the RNA-Induced Silencing Complex (RISC). This enzyme complex subsequently binds to its complementary mRNA sequence, mediating cleavage of the target mRNA and the suppression of the target protein encoded by the mRNA (Elbashir et al, 2001). Unmodified siRNAs are rapidly degraded by extra-and intracellular nucleases which limits tissue distribution upon systemic administration (Soutchek et al, 2004). Conjugation of the siRNA with N-acetylgalactosamine (GalNAc), which targets the asialoglycoprotein receptor (ASGPR), richly expressed on hepatocytes (Nair et al., 2014) has been successfully used as a delivery approach and leads to high levels of siRNA in hepatocytes. Multiple GalNAc-siRNAs have achieved proof-of-concept status in the clinic (Fitzgerald et al., 2017; Pasi et al., 2017; Zimmermann et al., 2017). Current GalNAc-siRNAs employ enhanced stabilization chemistry (ESC) (Foster et al., 2018), a design which confers increased stability against nuclease degradation resulting in enhanced potency, lower dose, less frequent dosing, and reduced exposure to monomers (Janas et al., 2019). The ESC chemistry and GalNAc delivery platform are used for several siRNA compounds currently in clinical development, including five that are in Phase 3 development (givosiran, fitusiran, inclisiran, lumasiran and vutrisiran), and one in Phase 2 (cemdisiran).

There is no regulatory DDI guidance for oligonucleotide therapeutics; as such, they are considered as small molecule drugs and evaluation of their potential for DDI is encouraged. To satisfy these recommendations, in vitro studies are typically carried out to evaluate whether a new chemical entity (NCE) is a substrate of CYPs or transporters, or if it can inhibit or induce major CYPs. Since there are well documented interactions due to inhibition of transporters, this

is also generally evaluated in vitro during drug development. While there are some differences in the interpretation of a positive DDI signal depending on the regulatory authority (EMA, 2012; FDA, 2017; PMDA, 2017), they are united in the recommendation for conducting in vitro experiments to derive the kinetic parameters to contextualize the clinical potential for DDI. EMA also specifically states that the potential for higher concentrations in the hepatocytes than in the plasma should be discussed, and if available data indicate that the drug may accumulate in hepatocytes, this should be considered in the AUCR estimations (EMA, 2012). These aspects are relevant for GalNAc-siRNAs given their targeted delivery to the liver.

In 2018, the first siRNA therapeutic, ONPATTRO® (patisiran) was approved. Patisiran is formulated as a lipid nanoparticle, and therefore, the mode of delivery to hepatocytes is different than GalNAc conjugated siRNAs which are the focus of this paper. GalNAc-siRNAs are ~16,000 kDa, highly soluble and negatively charged at physiological pH. They are rapidly taken up into the liver (target tissue) by ASGPR, where they are metabolized by endo- or exo-nucleases followed by subsequent excretion into bile or urine. Preclinical and clinical data suggest that renal clearance of intact GalNAc-siRNA accounts for less than 25% of the total clearance (unpublished, internal data). Given these attributes, it is highly unlikely that GalNAc-siRNA would serve as substrates or inhibitors/inducers of drug metabolizing enzymes and transporters. Additionally, given the mechanism of uptake and the rapid distribution into the liver, the circulating plasma levels are low and transient. Furthermore, the free intracellular hepatocyte concentration is also likely to be low since ASGPR-mediated endocytosis deposits the siRNA into the lysosomal compartment (Weigel and Yik, 2002). A recent publication evaluated the potential for antisense oligonucleotides (ASOs) to mediate DDI based on in vitro investigations (Shemesh et al., 2017), but there is no published data on GalNAc-siRNAs. As part of the nonclinical characterization, the DDI potential towards CYPs and transporters was evaluated for multiple GalNAc-siRNAs during their development. The assays conducted were dependent on the development stage for the GalNAc-siRNA, for example full transporter studies

were only conducted on those in late stage (Phase 2/3) development. These data indicate that the likelihood for clinical DDI at pharmacologically relevant doses is low.

Materials and Methods

GalNAc-siRNA

All oligonucleotides were synthesized as previously described by Nair et al (Nair et al., 2014). The general chemical modifications used in inclisiran, revusiran, fitusiran and givosiran have been previously published (Shen and Corey, 2018), the designs of all other GalNAc-siRNA are consistent with those already published with or without the addition of a glycol nucleic acid (GNA), (Schlegel et al., 2017).

Chemicals and Reagents Antipyrine, 2-Benzoxalinone, carbutamide, reserpine, warfarin, phenacetin, bupropion, paclitaxel, diclofenac, dextromethorphan, omeprazole, phenobarbital, rifampicin, Estrone-3-sufate sodium salt, taurocholic acid sodium salt, cyclosporin A, metformin, pyrimethamine, verapamil hydrochloride, probenecid, β-Estradiol 17-(β-D-glucuronide) sodium salt, cholecystokinine-8, β-Nicotinamide adenine dinucleotide phosphate reduced (NADPH), dimethylsulfoxide (DMSO), 1.0 M potassium phosphate monobasic solution, 1.0 M potassium phosphate dibasic solution were purchased from Sigma Chemicals (St. Louis, MO), midazolam and S-mephenytoin, 6α-hydroxypaclitaxel, 6α-hydroxypaclitaxel-d_5 and (±)-4-hydroxymephenytoin-d_3 were purchased from Toronto Research Chemicals (Toronto Canada), acetonitrile (MeCN) and methanol were purchased from Fisher scientific (Pittsburgh, PA). Recombinant human CYPs (rCYPs), ITS+ Premix and Matrigel™ were purchased from Corning (Tewksbury, MA). Pooled human liver microsomes (Lot No. 1210223, mixed gender, pool of 200 donors) were purchased from XenoTech, LLC (Lenexa, Kansas). Acetaminophen, hydroxybupropion, 4'-hydroxydiclofenac, 4'-hydroxymephenytoin, dextrorphan tartrate, 1'-hydroxymidazolam, 6β-hydroxytestosterone, acetaminophen-d_4, (±)-hydroxybupropion-d_6, 4'-hydroxydiclofenac-$^{13}C_6$, dextrorphan-d_3, 1'-hydroxymidazolam-d_4, and 6β-hydroxytestosterone-d_3 were purchased from Cerilliant (Round Rock, TX). 96-well polypropylene assay plates and rubber sealing mats were purchased from Fisher Scientific (Pittsburgh, PA). Ko124, 3H-N-methyl-quinidine, N-methyl-quinidine, and ^{3}H Estrone-3-sulfate were supplied by Solvo (Szeged,

Hungary). ^{3}H-Taurocholic acid, ^{3}H Estradiol 17 β-D glucuronide and ^{3}H-cholecystokinine-8 were supplied by Perkin Elmer (Waltham, MA). ^{3}H-tenofovir and ^{14}C metformin were supplied by Moravek biochemicals (Brea, CA), tenofovir was supplied by Sequoia research products Ltd.

Determination of incubation concentrations for in vitro assays

The concentrations of GalNAc-siRNAs used in the in vitro assays were selected by considering the observed plasma concentrations and estimated liver concentrations in the clinic (Table 1). Since GalNAc-siRNAs are large, anionic and hydrophilic in nature, they do not passively cross plasma membranes. These siRNAs do not bind to albumin (data on file) and are unlikely to bind to liver microsomes or hepatocytes. A recent publication evaluated the potential for a different design of chemically modified GalNAc-siRNA to bind to plasma and liver proteins (Humphreys et al., 2019). Their data indicated that binding to liver homogenate appeared greater than plasma binding, however these studies were designed with a final protein concentration of 200 mg/mL (personal communication with first author). This protein concentration is much greater than what was used during the in vitro DDI investigations of 0.1 to 1 mg/mL contained herein. If protein binding is estimated from this reported data (fu_{liver} = 0.018 to 0.051), with the assumption that binding to liver homogenate is linear with protein level, than the binding under the assay conditions employed (0.1 or 1 mg/mL) is expected to be negligible (fu_{liver} = 0.8 to 1). This approach has previously been published (Kalvass et al., 2007; Sane et al., 2016; Riccardi et al., 2017). Furthermore, the chemically modified GalNAc-siRNAs are highly stable in liver in vivo and are not expected to be appreciably metabolized during the short incubation times employed in the in vitro studies (Nair et al., 2017). Therefore, no corrections are made for metabolic stability, plasma protein binding (assumed to be 1) and K_i values estimated from IC_{50} values are expected to be representative of free values. It should be noted that the use of Fu = 1 is highly conservative as the PPB at relevant clinical concentrations is ~90% (Fu = 0.1).

CYP substrate study

Recombinant enzymes were thawed rapidly at 37°C and kept on ice until use per manufacturer's recommendation. Individual rCYP incubations contained 50 pmol/mL of rCYP1A2, rCYP2B6, rCYP2C8, rCYP2C9, rCYP2C19, rCYP2D6, rCYP3A4 or rCYP3A5, 2 concentrations of GalNAc-siRNA, or 1 µM CYP probe substrate. Reactions were initiated by the addition of NADPH (1 mM final concentration). Protein concentrations for all enzymes were normalized to the recombinant CYP containing the highest protein concentration (Supplemental Table 1). All reactions were carried out in triplicate and the final organic solvent concentration in the incubation was ≤1%. Reactions containing test article were terminated at 0 and 30 min by freezing on contact with dry ice/ethanol. Reactions containing positive controls were terminated by adding 100 µL aliquot of the reaction mixture to 100 µL of ice cold ACN containing a cocktail of internal standard (0.5 µM of reserpine, antipyrine, carbutamide, warfarin and 1 µM 2-benzoxazolinone). Probe substrates for each of the rCYP enzymes were included in the study as positive controls. The negative control incubations consisted of the test article with rCYPs but without NADPH. GalNAc-siRNA was analyzed by LC-TOF-MS. Positive control substrates were analyzed by UHPLC-MS/MS. Peak area ratios were used to calculate the percent parent remaining following 30- or 45-min incubations.

CYP direct and time dependent inhibition study

The substrate concentrations used were selected to approximate the K_m values, determined for each batch of HLMs used. Potassium phosphate buffer (100 mM, pH 7.4) was prepared by first diluting 1 M solutions of monobasic potassium phosphate and dibasic potassium phosphate with ultrapure water to 0.1 M. The 100 mM solutions were combined in a ratio (~3:1) dibasic:monobasic potassium phosphate such that the final pH of the buffer was 7.4. HLM at 20 mg/mL was diluted in the reaction mixture to 0.1 mg/mL for incubation with probe substrate. Probe substrate assay conditions were designed by considering linearity of reaction and ensuring that minimal (<10%) depletion of substrates occurred over the incubation time-course (characterization data on file at CRO). Reactions were started by the addition of 20 µL of 10

mM NADPH (10×) and returned to the incubated shaker. The total incubation volume was 200 µL. All incubations were conducted at 37°C. Reactions proceeded for 5 minutes (midazolam), 10 minutes (phenacetin, dextromethorphan, and testosterone), 15 minutes (bupropion, diclofenac), 25 minutes (*S*-mephenytoin), or 40 minutes (paclitaxel). At the end of incubation, 100 µL of each reaction was terminated with an equal volume of ice cold ACN containing a cocktail of stable labeled internal standards. Time-dependent inhibition of CYP activities were performed using pooled human liver microsomes with 30-minute pre-incubations. Pooled human liver microsomes (1 mg/mL) were pre-incubated for 30 minutes with GalNAc-siRNA (ten concentrations in triplicate) in KPi buffer in the presence or absence of 1 mM NADPH at 37°C. Reactions (50 µL) containing KPi, HLM, and NADPH were started with 12.5 µL of the 4× inhibitor dilution, blank or 4× positive control inhibitor. Mechanism based selective inhibitors furafylline (1 µM for CYP1A2), ThioTEPA (5 µM for CYP2B6), gemfibrozil glucuronide (25 µM for CYP2C8), tienilic acid (1 µM for CYP2C9), ticlopidine (10 µM for CYP2C19), paroxetine (0.5 µM for CYP2D6), and azamulin (0.5 µM for CYP3A4/5) were included as the positive controls in triplicate. Following the 30-minute pre-incubation time period a 20 µL aliquot was taken from each well and added to 180 µL of reaction mix. NADPH was approximately 1 mM and HLM was 0.1 mg/mL. The plates containing the substrate reactions were placed on the incubated shaker and proceeded for 5 minutes (midazolam), 10 minutes (phenacetin, dextromethorphan, testosterone), 15 minutes (bupropion, diclofenac), 25 minutes (*S*-mephenytoin), or 40 minutes (paclitaxel). At the end of incubation, reactions were terminated by mixing 100 µL of each reaction mixture with an equal volume of ice cold ACN containing a cocktail of stable labeled internal standards.

CYP induction study

Cryopreserved human hepatocytes from 3 different human donors were used for evaluation of induction potential. Donor demographics are located in Supplemental Table 2. Frozen vials of cryopreserved hepatocytes were rapidly thawed in a 37°C water bath and re-suspended in

Hepatocyte Plating Medium (HPM) containing ~30% Percoll. The cells were centrifuged and resuspended in HPM and the viability and cell count determined using the Nexcelom Cellometer according to the manufacturer's procedures. Cells were only used if the final isolation viability was greater than 80%. HPM was added to bring the cells to the required concentration and seeded onto 24-well plates coated with a simple collagen, type I substratum. Cells were incubated in a humidified chamber at 37°C, 5% CO_2 and cell attachment was confirmed 4 to 6 hours after plating by visual inspection using phase contrast microscopy. After attachment, plates were swirled, and medium containing debris and unattached cells was aspirated. Fresh HMM containing ITS+ Premix and Matrigel™ was added to culture plates and the plates were immediately returned to the humidified incubation chamber. Hepatocyte cultures were maintained for approximately 24 hours prior to treatment with GalNAc-siRNAs or prototypical inducers. Positive and negative controls were prepared at 1000× the final concentration in DMSO. Working solutions were prepared by dilution of the 1000× solutions in HMM (1 µL stock + 999 µL media). The final concentration of DMSO under all conditions was 0.1%. Cultures were treated for 2 or 3 consecutive days for RT-PCR or in situ activity, respectively, with solvent alone (0.1% DMSO), positive controls (50 µM OM, 1 mM PB and 10 µM RIF), negative control (25 µM FLUM), or test article. All treatments were carried out in triplicate. The medium was replaced daily with fresh supplemented medium containing the appropriate treatment. Prior to mRNA preparation at 48 hours of treatment or in situ CYP activity determination at 72 hours, 100 µL/well of culture supernatant was taken and assayed for lactate dehydrogenase (LDH) leakage using the CytoTox-ONE™ Homogeneous Membrane Integrity Assay kit (Promega, Madison, WI). After 48 hours of treatment, spent medium from a subset of each treatment group was aspirated and cells lysed for mRNA preparation with 200 µL of 1:1 Buffer RLT (Qiagen) and Trizol (Life Technologies). RNA was isolated using RNeasy Kit (Qiagen) according to the manufacturer's instructions. Eluted RNA was quantified using a Nanodrop spectrophotometer (ThermoFisher, Pittsburgh, PA). Reverse transcription (RT) was performed with the High

Capacity cDNA Reverse Transcriptase Kit with RNase inhibitor (Life Technologies, Carlsbad, CA) using an ABI 9700 thermocycler. Quantitative PCR analysis was performed on RT reactions using gene-specific primer/probe sets for CYP1A2, CYP2B6 or CYP3A4 target cDNA and endogenous control (GAPDH). Relative-fold change in mRNA content was determined based on threshold cycle (C_T) data of each target gene relative to endogenous control for each reaction and normalized to vehicle control. After 72 hours of treatment, the spent medium was aspirated from the remaining cultures from each treatment group, wells were washed with warmed HMM and a cocktail of CYP probe substrates in HMM was added to each well (phenacetin; 100 µM, bupropion; 50 µM, midazolam; 10 µM). Probe substrate incubations were performed for 30 min at 37°C on a rotary shaker at 150 RPM and terminated by taking 100 µL of the reaction and adding it to 100 µL/well of ice-cold acetonitrile with stable labeled internal standards. Plates were vortexed for 4 min and then centrifuged at 3000 RPM for 10 min at 4°C and then analyzed for quantitation of metabolite levels.

Evaluation of GalNAc-siRNA uptake into sandwich cultured hepatocytes

Cryopreserved human hepatocytes from a single donor were used to determine whether the human hepatocytes were exposed to GalNAc-siRNAs evaluated in the CYP induction study. Human hepatocytes were recovered, plated and cultured as described in the CYP induction study section. After the acclimation period the same concentrations of GalNAc-siRNAs used to evaluate induction potential were added to the hepatocytes. Twenty-four hours post GalNAc-siRNA administration hepatocyte cultures were washed twice with ice-cold PBS and 100 µL of lysis buffer containing 0.25% TritonX-100 in 1X PBS was added to lyse the cells. Cells were scraped from the bottom of the well and test article concentrations were determined. The concentration of test articles in the in vitro hepatocyte samples were determined using a RT-qPCR method capable of quantitating antisense strands of siRNA using a target-specific stem-loop primer and sequence-specific forward and reverse primers for amplification using the general conditions previously described (Landesman et al., 2010). PBS-TritonX-100 buffer was

spiked with test articles to generate the standard curves and quality control (QC) samples. Concentrated samples were diluted in 0.25% PBS-TritonX-100. Intracellular concentrations were estimated as previously described (Ramsden et al., 2014), using the viable seeded cell number of 65,000 cells/well.

In vitro transporter substrate study

Specific transporter assay details are presented in Supplemental Table 3. The accumulation of GalNAc-siRNA into membrane vesicles was determined using inside-out membrane vesicles (total protein: 50 µg/well for all transporters) prepared from cells overexpressing human ABC transporters as well as from control cells. Two incubation time points (2 and 20 min) and two concentrations of GalNAc-siRNA were tested in the presence of ATP or AMP, to determine whether GalNAc-siRNA is actively transported into the vesicles. Reactions were quenched by the addition of 200 µL of ice-cold washing buffer and immediate filtration via glass fiber filters mounted to a 96-well plate (filter plate). The filters were washed 5 × 200 µL of ice-cold washing buffer and dried. GalNAc-siRNA was extracted from the vesicles through lysing these by applying 2 times with 100 µL lysis solution (Epicentre, Tissue & Cell Lysis Solution (600 ml). Samples were analyzed to determine the concentration of GalNAc-siRNA retained inside the vesicles determined by LC-MS/MS detection. Incubation with AMP provided background activity values for all data points. Incubation with probe substrate (solvent only) served as positive controls while membrane vesicle preparations from control cells (for BCRP and P-gp) or Sf9 cells expressing beta-gal (for BSEP) served as negative controls.

In vitro transporter inhibition study - vesicular assays

GalNAc-siRNA was incubated with membrane vesicle preparations (total protein: 25 µg/well for BCRP and 50 µg/well for BSEP and P-gp) and the probe substrate. Incubations were carried out in the presence of 4 mM ATP or AMP to distinguish between transporter-mediated uptake and passive diffusion into the vesicles. GalNAc-siRNA was added to the reaction mixture in 1.5 µL of solvent. Reaction mixtures were preincubated for 10 minutes at 32 ± 1 °C for BCRP and at 37 ±

1 °C for BSEP and P-gp. Reactions were initiated by the addition of 25 µL of 12 mM MgATP (or 12 mM AMP in assay buffer as a background control), preincubated separately. Reactions were quenched by the addition of 200 µL of ice-cold washing buffer and immediate filtration via glass fiber filters mounted to a 96-well plate (filter plate). The filters were washed (5 × 200 µL of ice-cold washing buffer), dried and the amount of substrate inside the filtered vesicles was determined by liquid scintillation counting.

In vitro transporter substrate study - uptake assays

Uptake experiments were performed using CHO, MDCKII, or HEK293 cells stably expressing the respective uptake transporters. Cells were cultured at 37 ± 1 °C in an atmosphere of 95:5 air:CO2 as described in Supplemental Table 3 and were plated onto standard 24-well tissue culture plates at the density 5×10^5 cells/well. The uptake of GalNAc-siRNA was determined using cells overexpressing the respective uptake transporters (MATE1, MATE2-K, OAT1, OAT3, OATP1B1, OATP1B3, OCT1 and OCT2) and control cells, at two incubation time points (2 and 20 min) and at two concentrations of GalNAc-siRNA. In follow-up inhibition assays conducted for MATE1, OATP1B1 and OAT3, the transporter-specific uptake of GalNAc-siRNA was determined in the presence of a known inhibitor of the respective transporter (1 µM pyrimethamine for MATE1, 50 µM rifampicin for OATP1B1 and 200 µM probenecid for OAT3). Before the experiment, the medium was removed, and the cells were washed twice with 300 µL of HK buffer (pH 7.4 or 8.0). Cellular uptake of GalNAc-siRNA into the cells was measured by adding 300 µL of HK buffer containing GalNAc-siRNA and incubating them at 37 ± 1 °C. Reactions were quenched by removing the HK buffer containing GalNAc-siRNA and the cells were washed twice with 300 µL of HK buffer. Cells were lysed by adding 300 µL of lysis solution (Epicentre, Tissue & Cell Lysis Solution (600 ml) and incubated for 10 minutes. Samples were analyzed to determine the concentration of GalNAc-siRNA retained inside the vesicles determined by LC-MS/MS detection. The amount of protein in each well was quantified using the BCA kit for protein determination (Sigma-Aldrich, St Louis, MO, USA).

In vitro transporter inhibition study - uptake assays

Cells were cultured at 37 ± 1 °C in an atmosphere of 95:5 air: CO2 and were plated onto standard 96-well tissue culture plates at the cell number described in Supplemental Table 3. Before the experiment, the medium was removed, and the cells were washed twice with 100 µL of HK buffer at pH 7.4 (OAT1, OAT3, OATP1B1, OATP1B3, OCT1 and OCT2) or 8.0 (MATE1 and MATE2-K). Uptake experiments were carried out at 37 ± 1 °C in 50 µL of HK buffer (pH 7.4 or pH 8.0) containing the probe substrate and GalNAc-siRNA or solvent. The organic solvent concentration was equal in all wells. After the experiment, cells were washed twice with 100 µL of ice-cold HK buffer and lysed with 50 µL of 0.1 M NaOH. Radiolabeled probe substrate transport was determined by measuring an aliquot (35 µL) from each well for liquid scintillation counting. Uptake of the probe substrate in control cells provided background activity values for all data points. Incubation without GalNAc-siRNA or reference inhibitor (PBS only) provided 100% activity values. A reference inhibitor served as positive control for inhibition.

Analytical Methods Samples (20 µL) were injected on a Supelco Discovery C18 5µ 2.1x150 mm column maintained at room temperature using a Thermo Accela High Speed LC system. A solvent system consisting of water with 0.1% formic acid (mobile phase A) and acetonitrile with 0.1% formic acid (mobile phase B) was used at a flow rate of 0.4 mL/min was used with the following gradient: 0 – 5 min 15% B, 5 – 10 min 15 – 52.5% B, 15 – 16 min 52.5 – 85% B maintain 85% B for 2 min, 18 – 19 min 15% B then equilibrated for 3 min. The column eluent was analyzed by MS on a Thermo LTQ OrbiTrap XL Mass Spectrometer run in positive mode using FTMS and data-dependent FT MS/MS scans (CID and HCD) to elucidate metabolite structures. The resulting data were analyzed using Xcalibur 3.0 and Thermo Metworks 1.3 software.

Analysis of GalNAc-siRNA concentrations

LC-TOF-MS assays were developed. The LC-TOF-MS assays quantified the concentrations of specific GalNAc-siRNAs by peak area ratio (PAR), by detecting the antisense strand and sense

strand portion of the duplex (by PAR only). Incubation samples were spiked with internal standard, processed by solid phase extraction, and analyzed using reversed-phase UHPLC with Turbo Ion Spray TOF-MS detection. Accurate mass of ten ions for each strand of the analyte, sense and antisense, and each strand of IS, antisense and sense, were monitored in the negative ion mode. The peak area for the analyte or IS was the sum of the response from the respective ten ions. The peak area ratios of the respective analyte-sense/IS-sense and analyte-antisense/IS-antisense single strands were used.

Probe substrates CYP assays

The quenched reactions were vortexed at high speed (knob setting 10) for four minutes and centrifuged for 10 min at 3000 ± 40 x rpm at low temperature (~10°C). A portion of the supernatant (150 µL) was transferred into 1.4 mL snaplock tubes (Nova Biostorage). Samples were centrifuged for five min as described above prior to injection on the UHPLC-MS/MS. The analysis system consisted of a Shimadzu Nexera X2 LC-30 UPLC system (Shimadzu Corporation, Kyoto, Japan) and an API4000 triple quadrupole mass spectrometer (AB Sciex, Toronto, Canada). The LC-MS/MS system was controlled by Analyst software (version 1.6.1). Analyst performed the system hardware control and sample analysis. The following transitions were used for probe substrate assays. Phenacetin (180.12→138.17), acetaminophen (152.1→110.1), Bupropion (240.11→184.07), (±)-Hydroxybupropion (256.1→131.2), Paclitaxel (854.46→569.20), Diclofenac (296.32→214.07), S-Mephenytoin (219.19→134.09), Dextromethorphan (272.26→215.15), Midazolam (326.14→291.12), 1'-Hydroxymidazolam (342.1→203.1), internal standards warfarin (309.39→163.00), Acetaminophen-d_4 (156.1→114.1), 1'-Hydroxymidazolam-d_4 (346.1→203.1), Hydroxybupropion-d_6 (262.1→131.2).

Calculations and Data Analysis

IC_{50} values

Concentrations of the metabolites formed were calculated from a calibration curve using authentic metabolite standards. The CYP activities were expressed as pmol/min/mg of microsomes. The degree of inhibition was determined by comparing the formation of metabolites in the presence of different concentrations of GalNAc-siRNA versus vehicle control. IC_{50} values were calculated from the percent vehicle control activity using Prism 7 for Windows (GraphPad Software, La Jolla, CA) and applying Equation 1. Comparison of three parameter (hillslope = -1) or four parameter fitting was conducted to determine the best fit. Curve fitting was not carried out in cases where the inhibition at the highest concentration of test article was ≤ 10% of the control value, rather the IC_{50} value was set to > the highest concentration of GalNAc-siRNA tested. The calculated IC_{50} values for positive controls were compared with reported literature values and results typically obtained at QPS.

Equation 1 $$Y = min + \frac{max - min}{1 + (\frac{x}{IC_{50}})^{-hillslope}}$$

To determine if the test article is a time-dependent inhibitor, changes in IC_{50} value from pre-incubated samples with NADPH were compared to IC_{50} value from samples pre-incubated without NADPH. Time-dependent inhibition was indicated if the ratio of IC_{50} (without NADPH)/IC_{50} (with NADPH) is > 1.5 (Grimm et al., 2009). For the assay to be considered valid the time-dependent controls had to cause at least a 20% change in the % inhibition in the presence of NADPH.

K_i values were estimated from IC_{50} values using the Cheng-Prusoff equation (Cheng and Prusoff, 1973) assuming a competitive inhibition mechanism:

$$IC_{50} = K_i \cdot \left(1 + \frac{[S]}{K_m}\right)$$

Induction data

TaqMan® data was analyzed using the comparative C_T method (Schmittgen and Livak, 2008) (also known as the $\Delta\Delta C_T$ method). The C_T values from the samples and the GAPDH controls were used for the calculations. The ΔC_T was calculated by subtracting the C_T of the reference (GAPDH) from the C_T value of the sample. Next the $\Delta\Delta C_T$ value was calculated by subtracting the mean ΔC_T of the calibrator (the vehicle control) from each sample ΔC_T. The relative quantitation (or fold over control) was calculated by raising 2 to the negative power of the $\Delta\Delta C_T$.

Statistical analyses

The means of all replicates were used in calculations. IC_{50} values were determined using GraphPad Prism (version 7) (GraphPad Software, La Jolla, CA). Data were processed with Microsoft Excel 2010 (Microsoft, Redmond, WA). To evaluate significance for induction studies data was analyzed using one-way ANOVA with the results examined for statistical significance using the Bonferroni procedure in XLSTAT add-in for Microsoft Excel® (Addinsoft, New York, NY). When necessary, data was examined for outliers using the Grubb's test (Grubbs F.E, 1950). The 'Grubbs test for Outliers' module of XLSTAT add-in for Microsoft Excel® (Addinsoft, New York, NY) was used to perform the analysis. All studies were conducted at QPS (Newark, DE), Solvo (Szeged, Hungary), or Sekisui XenoTech (Kansas City, KS) in accordance with company specific standard operating procedures (SOP), in the spirit of GLP.

Estimation of liver concentrations in human

The maximal concentration in human liver was estimated using Phoenix WinNonlin and two approaches. The first considered the relationship between rat and monkey liver to plasma ratios where the monkey liver to plasma ratio was scaled allometrically to human based on body weight with an exponent of 0.37. The exponent was derived using the average mouse, rat and monkey liver to plasma ratios determined at non-saturating dose levels of nine GalNAc-siRNAs during PK/PD studies. The second approach relied on simulations derived from fitting of the average liver PK profile observed in monkey and allometric scaling CL (exponent 0.75) and V

(exponent 1). The estimated liver concentrations were within 2.5-fold of each other using all methods and the mean concentration was used as an input for the DDI risk assessment. The estimated liver concentrations are based on total concentrations and not reflective of free concentrations, or discriminative of location (i.e. hepatocytes, endocytic pathway vs endoplasmic reticulum).

Mechanistic static modeling

The mechanistic static model reported previously (Fahmi et al., 2009) was used with the following exceptions. Equation 1 was reduced to Equation 2 considering the enzymes inhibited, the mode of GalNAc-siRNA delivery (subcutaneous rather than oral) and the interactions observed (direct inhibition only).

$$\mathrm{AUCi/AUC} = \left(\frac{1}{[A_h \times B_h \times C_h] \times f_m + (1 - f_m)}\right) X \left(\frac{1}{[A_g \times B_g \times C_g] \times (1 - f_g) + f_g}\right) \quad \text{Equation 1}$$

$$\mathrm{AUCi/AUC} = \left(\frac{1}{[A_h] \times f_m + (1 - f_m)}\right) \quad \text{Equation 2}$$

Where

$$A_h = \frac{1}{1 + \frac{[I]_h}{K_i}}$$

I = estimated liver concentration (Table 1)

Results

CYP substrate

The potential of GalNAc-siRNAs to act as a substrate of major CYP isoforms was evaluated using cDNA expressed enzymes (refer Table 2). In vitro incubations were conducted in triplicate with two concentrations each of seven GalNAc-siRNAs which contain different oligonucleotide sequences and chemical modifications. No NADPH dependence and no meaningful depletion of the GalNAc-siRNAs was observed after incubation with recombinant enzymes (Table 2). These studies were designed to evaluate both the sense and antisense strands. The positive control substrates all resulted in time-dependent depletion over the incubation time-course, which was consistent with historical data, confirming that rCYPs were appropriately functional (Supplemental Table 4). Based on the minimal depletion observed, GalNAc-siRNAs are not substrates of CYP 1A2, 2B6, 2C8, 2C9, 2C19, 2D6, 3A4, or 3A5, and therefore, clinical interactions with inhibitors and inducers of CYP enzymes are not likely.

CYP direct and time dependent inhibition

The potential of twelve GalNAc-siRNAs to inhibit the major CYP isoforms (ie, CYP1A2, CYP2B6, CYP2C8, CYP2C9, CYP2C19, CYP2D6, and CYP3A) was evaluated in vitro using pooled human liver microsomes (HLM), standard probe substrates for each CYP isoform and included appropriate positive and negative controls. No direct or time dependent inhibition was observed for CYPs 1A2, 2C9, 2C19, 2D6 or 3A4/5 by any of the GalNAc-siRNAs evaluated (Figure 1, Table 3). AAT02 was also evaluated for time-dependent inhibition and resulted in an IC_{50} value > 18.4 µM with and without NADPH for the same CYPs (data not included in table). Additionally, although not requested to be evaluated by regulatory authorities, fitusiran did not result in direct inhibition of CYP2A6. All prototypical direct and time-dependent inhibitors resulted in values in line with literature reports (Supplemental Tables 5 and 6), demonstrating

that the test system was functional for assessing inhibition potential. Cemdisiran, fitusiran and lumasiran resulted in direct inhibition of CYP2C8 at very high incubation concentrations with IC_{50} values of 224, 56 and 416 µM, respectively. These values are > 4,600-fold higher than the total maximal steady state concentrations observed in plasma. Cemdisiran also caused concentration dependent direct inhibition of CYP2B6 with an IC_{50} value of 583 µM, which is 12,000-fold higher than the therapeutically relevant plasma $C_{max,ss,total}$. No time-dependent inhibition was observed for CYP2C8 or CYP2B6 by any of the GalNAc-siRNAs tested. Considering the in vitro data and the recommendations in regulatory guidance documents (FDA 2017; EMA 2012) the risk of clinical DDI due to inhibition is low.

CYP induction

No concentration dependent or statistically significant increase in mRNA levels was observed for any of the GalNAc-siRNAs evaluated while the positive and negative control compounds elicited expected magnitudes of response (Figure 2). There were also no measurable increases in enzyme activity following any of the GalNAc-siRNA treatments (data on file). Metabolic stability for inclisiran was determined during the induction study and results demonstrated that inclisiran was highly stable (<5% depletion) over the 24-hour exposure period (Table 4).

Confirmation of uptake into sandwich cultured hepatocytes

Higher concentrations of GalNAc-siRNAs were observed in hepatocytes than the nominal incubation concentrations, particularly at lower concentrations (Table 5). This is consistent with the knowledge that ASGPR mediates active uptake of GalNAc into hepatocytes. The saturation of ASGPR uptake is not unexpected at these concentrations and has been previously described (Bon et al., 2017). Taken together these data confirm that lack of induction during the in vitro induction study is not due to lack of exposure to test article.

Transporter substrate

Four GalNAc-siRNAs were evaluated as potential substrates of uptake (OATP1B1, OATP1B3, OAT1, OAT3, OCT1 and OCT2) and efflux (BCRP, BSEP, MATE1, MATE2-K and P-gp) transporters. No significant accumulation >2-fold or inhibition of uptake by selective inhibitors >50% was observed for any of the GalNAc-siRNAs tested against any of the transporters evaluated. One potential exception was fitusiran which during an initial investigation was flagged as a potential substrate of MATE2-K based on the accumulation ratio (>2-fold). A follow up study showed an accumulation ratio for MATE2-K as <2-fold, but a mild inhibition when a prototypical MATE2-K inhibitor was used. Given the variability observed between studies, the knowledge that substrates for MATE2-K are typically cations and are generally also transported by OCT2 (Yonezawa and Inui, 2011), and that fitusiran was not a substrate for OCT2, the in vitro data was deemed inconclusive. Furthermore, considering that the fraction of fitusiran excreted in urine from hemophilia patients after 3 monthly doses was 17% of the total administered drug and no active secretion was observed this in vitro observation is likely not clinically relevant. Based on the totality of data the likelihood for GalNAc-siRNAs to act as substrates for transporters is low.

Transporter inhibition

The potential for GalNAc-siRNA to inhibit uptake (OATP1B1, OATP1B3, OAT1, OAT3, OCT1 and OCT2) and efflux (BCRP, BSEP, MATE1, MATE2-K and P-gp) transporters was assessed using transfected cell lines or vesicles expressing the transporter of interest. No significant inhibition was observed for uptake transporters or efflux transporters, with the exception of concentration dependent inhibition of P-gp by givosiran (Figure 3). While a full concentration effect curve was not generated, an estimation of the IC_{50} (4.2 µM) was made for the purpose of

conducting a clinical DDI risk assessment. This evaluation demonstrated that the in vitro inhibition of P-gp observed is not projected to be clinically relevant.

Estimation of total human liver concentrations

Since it is known that GalNAc-siRNA liver concentrations are much higher than the plasma concentrations in nonclinical animal models, it is expected that the liver levels are likewise going to be higher in human, although they cannot be directly measured. EMA recommend in these cases to consider the liver concentration for DDI assessment as a worst-case method (EMA 2012). Considering this, the human relevant maximal liver concentrations were estimated from the nonclinical animal data and used for modeling DDI potential. The relationship between rat and monkey preferential liver distribution (liver C_{max}/plasma C_{max}) is displayed in Figure 4. The values were positively correlated with monkey liver enrichment being greater than rat liver enrichment values for all GalNAc-siRNAs investigated. The mean estimated liver concentrations from in vitro data and two-approaches for modeling are displayed in Table 1. These values represent the total estimated liver concentration, and therefore, are considered to be the worst-case scenario. Given that ASGPR mediates uptake through endocytosis into the lysosomal compartment, it is expected that the free intracellular concentration available to interact with the drug metabolizing enzymes located in the endoplasmic reticulum is much less than the total estimated liver concentration. The total liver concentration was estimated to be between 50- and 870-fold higher than the plasma concentration across the six GalNAc-siRNA conjugates used to inform the model.

Clinical DDI risk assessment

Evaluation of GalNAc-siRNAs as perpetrators of DDI against CYP

GalNAc-siRNAs did not cause in vitro induction or time-dependent inhibition of CYPs; therefore, clinically relevant induction or time-dependent inhibition is not expected. One GalNAc-siRNA (cemdisiran) caused concentration dependent inhibition of CYP2B6 and three GalNAc-siRNAs (fitusiran, cemdisiran and lumasiran) caused concentration dependent inhibition of CYP2C8 at supratherapeutic concentrations. Based on these observations, a clinical risk assessment was made for CYP2B6 and CYP2C8 inhibition potential which was consistent with recommendations made in regulatory guidelines (EMA, FDA and PMDA), reference Table 6. All of the regulatory agencies are aligned in the cut-off criterion used for evaluating CYP inhibition potential. Namely that clinical risk cannot be excluded if the R1 value is > 1.02, where R1 = 1 + I/Ki and I is unbound $C_{max,ss}$. Given that GalNAc-siRNA are targeted to the liver, the estimated liver concentrations were also used as a worst-case evaluation, and a cutoff of R1 > 1.1 was applied. It should be noted that the regulatory guidance documents do not have recommendations for cut-off criteria when using input concentrations other than plasma. However, the highly conservative cut-off of 1.02 is recommended with the goal of avoiding false negatives by accounting for inherent system variability and/or accumulation at the interaction site. Using estimated liver concentrations represents a conservative approach beyond using unbound plasma concentrations and therefore, the cut-off was set to be 1.1, which is still below the threshold of clinically relevant inhibition (1.25). When the R1 value is > 1.02 (plasma) or 1.1 (liver), a second-tier approach can be used which includes modeling the potential with either a mechanistic static (net effect) or dynamic (PBPK) model. If the second-tier model is ≥ 1.25, then clinical evaluation would be recommended. Using the plasma concentration, the risk of clinically relevant inhibition of CYP2B6 or CYP2C8 is low. When using the liver concentration, the potential for clinically relevant inhibition of CYP2C8 by fitusiran and cemdisiran could not be excluded by the R1 equation, and therefore mechanistic static modeling was conducted. The substrate used in the modeling was cerivastatin (F_m = 0.82) which is more sensitive towards CYP2C8 than other substrates (i.e. repaglinide, F_m = 0.49-0.63). Using this approach, the

potential for clinically relevant DDI of CYP2C8 is low (R < 1.25) and no clinical interaction studies are warranted.

Givosiran as a P-gp inhibitor

The current FDA and PMDA draft DDI guidance documents propose a cut-off based only on orally administered drugs and recommend using $I_{gut}/IC_{50} > 10$. The route of administration for GalNAc-siRNAs is through subcutaneous injection, thus the potential for GalNAc-siRNAs to mediate gut level DDI on P-gp is low. For this reason, the cut-off of $I_1/IC_{50} \geq 0.03$ proposed by (Ellens et al., 2013, V Arya et al., 2017) was used to determine whether in vitro inhibition of P-gp by givosiran could be clinically relevant. Based on this analysis the likelihood for givosiran to inhibit P-gp in the clinic is very low (AUCR = 1.0).

Discussion

Regulatory authorities encourage thorough investigation of DDI potential during drug development since it can lead to adverse clinical effects or reduction in efficacy. These investigations are often carried out in vitro and are typically focused on the major drug metabolizing enzymes (CYPs and UGTs) and transporters where clinically relevant DDI has been observed. There is currently no guidance addressing DDI potential of novel therapeutics such as oligonucleotides. Therefore, recommendations made for small molecules are often adhered to during their development. Years of experience has enabled the recommendation that DDI of protein therapeutics, can be determined on a case by case basis (Huang et al., 2010), since DDI potential is low with the exception of cytokine modulators (Kenny et al., 2013). The rapid development of novel therapeutics containing oligonucleotides has resulted in many clinical studies over the last 30 years when the first ASO, fomivirsen was approved. An additional five ASOs have been approved and include, pegaptanib in 2004, mipomersen in 2013, eteplirsen, defibrotide, nusinersen in 2016 and inotersen in 2018. During this timeframe no significant pharmacokinetic DDI have been reported (Geary et al., 2002; Geary et al., 2006; Yu et al., 2009; Li et al., 2014). The first siRNA, ONPATTRO® (patisiran), approved by the FDA in 2018, employs a different dosing route and delivery mechanism than the current generation of GalNAc-siRNAs which are the focus of this paper.

Considering the mechanism of action, disposition, and molecular size, it is unlikely that GalNAc-siRNA would interact with drug metabolizing enzymes and transporters. They are highly soluble in water and negatively charged at physiological pH. ASGPR-mediated uptake efficiently delivers GalNAc-siRNA to the liver; thus, solute carrier transporters are unlikely to contribute to their active uptake. In nonclinical models (rat and monkey), renal clearance is not a major route of elimination of GalNAc-siRNA (less than 25% of total clearance) suggesting that the role of renal transporters is likely minor. Metabolite identification studies indicate that

GalNAc-siRNAs are metabolized to shortmers by exo- and endonucleases. GalNAc-siRNAs do not induce cytokines in vitro or in vivo, therefore, modulation of drug metabolizing activity through this mechanism is unlikely.

Reaction phenotyping of seven GalNAc-siRNAs confirmed that they are not substrates of CYP enzymes including, CYP 1A2, 2A6, 2B6, 2C8, 2C9, 2C19, 2D6, 3A4 and 3A5. Clinical interactions with inhibitors or inducers of CYP enzymes would therefore not be expected. None of the nine GalNAc-siRNAs tested caused any time-dependent inhibition of the major CYP enzymes including, CYP 1A2, 2A6, 2B6, 2C8, 2C9, 2C19, 2D6, 3A4 and 3A5. Mild direct inhibition was observed for CYP2B6 with cemdisiran (K_i = 292 µM) and for CYP2C8 with cemdisiran (K_i = 112 µM), fitusiran (K_i = 28 µM) and lumasiran (K_i = 208 µM). A recent publication by Sekisui XenoTech postulated that the phosphorothioate (PS) linkages, contained within the evaluated ASOs, could be the reason for observed direct inhibition of CYP in HLMs, which tended to be rank ordered as CYP1A2 ≈ CYP2C8 > CYP2B6 (Kazmi et al., 2018). The authors demonstrated test system dependency whereby inhibition studies carried out using a more physiologically relevant hepatocyte model resulted in no or reduced extents of inhibition. Unlike the ASO molecules which contain at least twelve PS linkages, GalNAc-siRNAs contain a maximum of six PS linkages. To evaluate the clinical relevance of CYP2B6 or CYP2C8 in vitro inhibition, a risk assessment using the decision trees presented in regulatory DDI guidance documents was performed. Since GalNAc-siRNAs are efficiently delivered to the hepatocytes via ASGPR, the liver concentration is anticipated to be much higher than plasma. However, as previously mentioned, the free intracellular concentration available to inhibit CYP enzymes on the endoplasmic reticulum is likely to be much lower than the total liver concentration. A worst-case assessment of DDI potential was made by inputting estimated total liver concentrations, in addition to plasma, to project the clinical outcome. Based on this analysis, no clinical DDI evaluation would be triggered (R value < 1.25). It is possible that conducting inhibition studies

using a more physiologically representative model such as hepatocytes, similarly to ASO, would yield lower extents of inhibition. However, since clinically relevant inhibition is not expected, these studies were not conducted.

There was no modulation of drug metabolizing enzymes observed during in vitro induction studies characterizing endpoints of AhR, CAR and PXR. Thus, clinical interactions due to induction of drug metabolizing enzymes by GalNAc-siRNA are unlikely. Taken together the likelihood for GalNAc-siRNA to perpetrate DDI against CYP substrates is unlikely.

Transporters can drive intracellular concentrations and mediate clinically relevant DDI; thus, regulatory agencies, EMA, FDA and PMDA recommend that all new chemical entities (NCE) be evaluated as substrates or inhibitors of transporters. In vitro investigations can be prioritized based on knowledge of the NCE as well as the physiochemical properties. For example, compounds with high solubility or permeability do not need to be evaluated as substrates of P-gp and BCRP and renal transporters only need to be evaluated if renal excretion is a major elimination pathway (EMA, 2012 and FDA, 2018). Inhibition of P-gp and BCRP should also be considered only for those molecules administered orally. The rationale for this is because clinically relevant DDI are more likely to occur at the GI tract where inhibitor concentrations would be much higher than plasma and therefore can achieve a high enough level to inhibit intestinal P-gp. A review of clinical DDI studies with common P-gp substrates (digoxin, dabigatran, loperamide and apixaban) yielded 249 total clinical interaction studies. Of these, 130 studies were positive for inhibition and all precipitants were dosed orally. Only 10 clinical DDI studies have been conducted to date with perpetrators dosed subcutaneously (5) or IV (5), and none of these studies resulted in relevant clinical inhibition. Clinical P-gp DDI studies with drugs administered subcutaneously were limited to GLP-1 receptor agonists (albiglutide, dulaglutide, lixisenatide, semaglutide) because of an on-target delayed gastric emptying which could alter GI absorption kinetics of co-administered therapies. The route of

administration for GalNAc-siRNAs is through subcutaneous injection, thus the potential for GalNAc-siRNAs to mediate gut level DDI on P-gp is low. The likelihood for givosiran to result in clinically meaningful inhibition of P-gp was determined to be low when considering the in vitro derived IC_{50} value. Current data across GalNAc-siRNAs demonstrate low potential for inhibition interactions with transporters. Furthermore, GalNAc-siRNAs were determined to not be substrates of clinically relevant transporters. Overall, these data confirm that the likelihood for clinically relevant interactions with transporters by GalNAc-siRNAs is low.

The totality of data confirms that chemical inhibition or induction of drug metabolizing enzymes and transporters mediated by GalNAc-siRNA is highly unlikely. The potential for pharmacological mediated DDI should be evaluated by understanding the mechanism of action and downstream or upstream effects of target gene knockdown. A weight of evidence approach for including/excluding clinical DDI investigation dependent on the properties of the siRNA and the pharmacology of the target is recommended. To reduce off-target effects, siRNA sequences are carefully designed, with the first step employing algorithms aimed to reduce the probability of perfect matches and hybridization with RNAs for genes other than the target followed by a strategy to mitigate off-target activity. In general, based on this large dataset, in the absence of any pathway mediated DDI potential, it can be concluded that GalNAc-siRNAs are unlikely to be a victim or perpetrator of DDI and *in vitro* or clinical investigations are not warranted.

Acknowledgements

The authors would like to thank Bahru Habtemariam, Martin Maier, Vasant Jadhav, Gabriel Robbie and Sara Nochur for thoughtful discussions and critical review of the manuscript.

Authorship Contributions

Participated in research design: Diane Ramsden, Jing-Tao Wu, Brad Zerler, Sajida Iqbal, Jim Jiang, Valerie Clausen and Saeho Chong

Conducted Experiments: Krishna Aluri, Yongli Gu, Sean Dennin, Joohwan Kim

Performed data analysis: Diane Ramsden

Wrote or contributed to the writing of the manuscript: Diane Ramsden, Jing-Tao Wu and Saeho Chong

References

Bon C, Hofer T, Bousquet-Melou A, Davies MR, and Krippendorff BF (2017) Capacity limits of asialoglycoprotein receptor-mediated liver targeting. *MAbs* **9:**1360-1369.

Cheng Y and Prusoff WH (1973) Relationship between the inhibition constant (K1) and the concentration of inhibitor which causes 50 per cent inhibition (I50) of an enzymatic reaction. *Biochem Pharmacol* **22:**3099-3108.

EMA (2012) Guideline of the investigation of drug interactions (Products CfHM ed.

Fahmi OA, Hurst S, Plowchalk D, Cook J, Guo F, Youdim K, Dickins M, Phipps A, Darekar A, Hyland R, and Obach RS (2009) Comparison of different algorithms for predicting clinical drug-drug interactions, based on the use of CYP3A4 in vitro data: predictions of compounds as precipitants of interaction. *Drug Metab Dispos* **37:**1658-1666.

FDA (2017) In Vitro Metabolism-and Transporter-Mediated Drug-Drug Interaction Studies Guidance for Industry (U.S. Department of Health and Human Services Food and Drug Administration Center for Drug Evaluation and Research CP ed.

Fitzgerald K, Kallend D, and Simon A (2017) A Highly Durable RNAi Therapeutic Inhibitor of PCSK9. *N Engl J Med* **376:**e38.

Foster DJ, Brown CR, Shaikh S, Trapp C, Schlegel MK, Qian K, Sehgal A, Rajeev KG, Jadhav V, Manoharan M, Kuchimanchi S, Maier MA, and Milstein S (2018) Advanced siRNA Designs Further Improve In Vivo Performance of GalNAc-siRNA Conjugates. *Mol Ther* **26:**708-717.

Geary RS, Bradley JD, Watanabe T, Kwon Y, Wedel M, van Lier JJ, and VanVliet AA (2006) Lack of pharmacokinetic interaction for ISIS 113715, a 2'-0-methoxyethyl modified antisense oligonucleotide targeting protein tyrosine phosphatase 1B messenger RNA, with oral antidiabetic compounds metformin, glipizide or rosiglitazone. *Clin Pharmacokinet* **45:**789-801.

Geary RS, Henry SP, and Grillone LR (2002) Fomivirsen: clinical pharmacology and potential drug interactions. *Clin Pharmacokinet* **41:**255-260.

Grimm SW, Einolf HJ, Hall SD, He K, Lim HK, Ling KH, Lu C, Nomeir AA, Seibert E, Skordos KW, Tonn GR, Van Horn R, Wang RW, Wong YN, Yang TJ, and Obach RS (2009) The conduct of in vitro studies to address time-dependent inhibition of drug-metabolizing enzymes: a perspective of the pharmaceutical research and manufacturers of America. *Drug Metab Dispos* **37:**1355-1370.

Huang SM, Zhao H, Lee JI, Reynolds K, Zhang L, Temple R, and Lesko LJ (2010) Therapeutic protein-drug interactions and implications for drug development. *Clin Pharmacol Ther* **87:**497-503.

Humphreys SC, Thayer MB, Lade JM, Wu B, Sham K, Basiri B, Hao Y, Huang X, Smith R, and Rock BM (2019) Plasma and liver protein binding of GalNAc conjugated siRNA. *Drug Metab Dispos*.

Janas MM, Zlatev I, Liu J, Jiang Y, Barros SA, Sutherland JE, Davis WP, Liu J, Brown CR, Liu X, Schlegel MK, Blair L, Zhang X, Das B, Tran C, Aluri K, Li J, Agarwal S, Indrakanti R, Charisse K, Nair J, Matsuda S, Rajeev KG, Zimmermann T, Sepp-Lorenzino L, Xu Y, Akinc A, Fitzgerald K, Vaishnaw AK, Smith PF, Manoharan M, Jadhav V, Wu JT, and Maier MA (2019) Safety evaluation of 2'-deoxy-2'-fluoro nucleotides in GalNAc-siRNA conjugates. *Nucleic Acids Res* **47:**3306-3320.

Kalvass JC, Maurer TS, and Pollack GM (2007) Use of Plasma and Brain Unbound Fractions to Assess the Extent of Brain Distribution of 34 Drugs: Comparison of Unbound Concentration Ratios to in Vivo P-Glycoprotein Efflux Ratios. **35:**660-666.

Kazmi F, Yerino P, McCoy C, Parkinson A, Buckley DB, and Ogilvie BW (2018) An Assessment of the In Vitro Inhibition of Cytochrome P450 Enzymes, UDP-Glucuronosyltransferases,

and Transporters by Phosphodiester- or Phosphorothioate-Linked Oligonucleotides. *Drug Metab Dispos* **46:**1066-1074.

Kenny JR, Liu MM, Chow AT, Earp JC, Evers R, Slatter JG, Wang DD, Zhang L, and Zhou H (2013) Therapeutic protein drug-drug interactions: navigating the knowledge gaps-highlights from the 2012 AAPS NBC Roundtable and IQ Consortium/FDA workshop. *AAPS J* **15:**933-940.

Kim D and Rossi J (2008) RNAi mechanisms and applications. *Biotechniques* **44:**613-616.

Landesman Y, Svrzikapa N, Cognetta A, Zhang X, Bettencourt BR, Kuchimanchi S, Dufault K, Shaikh S, Gioia M, Akinc A, Hutabarat R, and Meyers RJS (2010) In vivo quantification of formulated and chemically modified small interfering RNA by heating-in-Triton quantitative reverse transcription polymerase chain reaction (HIT qRT-PCR). **1:**16.

Li Z, Hard ML, Grundy JS, Singh T, von Moltke LL, and Boltje I (2014) Lack of clinical pharmacodynamic and pharmacokinetic drug-drug interactions between warfarin and the antisense oligonucleotide mipomersen. *J Cardiovasc Pharmacol* **64:**164-171.

Nair JK, Attarwala H, Sehgal A, Wang Q, Aluri K, Zhang X, Gao M, Liu J, Indrakanti R, Schofield S, Kretschmer P, Brown CR, Gupta S, Willoughby JLS, Boshar JA, Jadhav V, Charisse K, Zimmermann T, Fitzgerald K, Manoharan M, Rajeev KG, Akinc A, Hutabarat R, and Maier MA (2017) Impact of enhanced metabolic stability on pharmacokinetics and pharmacodynamics of GalNAc-siRNA conjugates. *Nucleic Acids Res* **45:**10969-10977.

Nair JK, Willoughby JL, Chan A, Charisse K, Alam MR, Wang Q, Hoekstra M, Kandasamy P, Kel'in AV, Milstein S, Taneja N, O'Shea J, Shaikh S, Zhang L, van der Sluis RJ, Jung ME, Akinc A, Hutabarat R, Kuchimanchi S, Fitzgerald K, Zimmermann T, van Berkel TJ, Maier MA, Rajeev KG, and Manoharan M (2014) Multivalent N-acetylgalactosamine-conjugated siRNA localizes in hepatocytes and elicits robust RNAi-mediated gene silencing. *J Am Chem Soc* **136:**16958-16961.

Pasi KJ, Rangarajan S, Georgiev P, Mant T, Creagh MD, Lissitchkov T, Bevan D, Austin S, Hay CR, Hegemann I, Kazmi R, Chowdary P, Gercheva-Kyuchukova L, Mamonov V, Timofeeva M, Soh CH, Garg P, Vaishnaw A, Akinc A, Sorensen B, and Ragni MV (2017) Targeting of Antithrombin in Hemophilia A or B with RNAi Therapy. *N Engl J Med* **377:**819-828.

PMDA (2017) Guideline of drug interaction studies for drug development and appropriate provision of information.

Ramsden D, Tweedie DJ, Chan TS, Taub ME, and Li Y (2014) Bridging in vitro and in vivo metabolism and transport of faldaprevir in human using a novel cocultured human hepatocyte system, HepatoPac. *Drug Metab Dispos* **42:**394-406.

Riccardi K, Lin J, Li Z, Niosi M, Ryu S, Hua W, Atkinson K, Kosa RE, Litchfield J, and Di L (2017) Novel Method to Predict In Vivo Liver-to-Plasma K_{puu} for OATP Substrates Using Suspension Hepatocytes. **45:**576-580.

Sane RS, Ramsden D, Sabo JP, Cooper C, Rowland L, Ting N, Whitcher-Johnstone A, and Tweedie DJ (2016) Contribution of Major Metabolites toward Complex Drug-Drug Interactions of Deleobuvir: In Vitro Predictions and In Vivo Outcomes. **44:**466-475.

Schlegel MK, Foster DJ, Kel'in AV, Zlatev I, Bisbe A, Jayaraman M, Lackey JG, Rajeev KG, Charisse K, Harp J, Pallan PS, Maier MA, Egli M, and Manoharan M (2017) Chirality Dependent Potency Enhancement and Structural Impact of Glycol Nucleic Acid Modification on siRNA. *J Am Chem Soc* **139:**8537-8546.

Schmittgen TD and Livak KJ (2008) Analyzing real-time PCR data by the comparative C(T) method. *Nat Protoc* **3:**1101-1108.

Shemesh CS, Yu RZ, Warren MS, Liu M, Jahic M, Nichols B, Post N, Lin S, Norris DA, Hurh E, Huang J, Watanabe T, Henry SP, and Wang Y (2017) Assessment of the Drug Interaction Potential of Unconjugated and GalNAc3-Conjugated 2'-MOE-ASOs. *Mol Ther Nucleic Acids* **9:**34-47.

Shen X and Corey DR (2018) Chemistry, mechanism and clinical status of antisense oligonucleotides and duplex RNAs. *Nucleic Acids Res* **46:**1584-1600.

Weigel PH and Yik JH (2002) Glycans as endocytosis signals: the cases of the asialoglycoprotein and hyaluronan/chondroitin sulfate receptors. *Biochim Biophys Acta* **1572:**341-363.

Yonezawa A and Inui K (2011) Importance of the multidrug and toxin extrusion MATE/SLC47A family to pharmacokinetics, pharmacodynamics/toxicodynamics and pharmacogenomics. *Br J Pharmacol* **164:**1817-1825.

Yu RZ, Geary RS, Flaim JD, Riley GC, Tribble DL, vanVliet AA, and Wedel MK (2009) Lack of pharmacokinetic interaction of mipomersen sodium (ISIS 301012), a 2'-O-methoxyethyl modified antisense oligonucleotide targeting apolipoprotein B-100 messenger RNA, with simvastatin and ezetimibe. *Clin Pharmacokinet* **48:**39-50.

Zimmermann TS, Karsten V, Chan A, Chiesa J, Boyce M, Bettencourt BR, Hutabarat R, Nochur S, Vaishnaw A, and Gollob J (2017) Clinical Proof of Concept for a Novel Hepatocyte-Targeting GalNAc-siRNA Conjugate. *Mol Ther* **25:**71-78.

Legends for Figures

Figure 1: The potential for a. cemdisiran, b. HBV01, c. vutisiran, d. AAT, e. fitusiran, f. givosiran, g. revusiran, h. lumasiran, i. inclisiran, j. AGT01, k. AAT02 or l. HBV02 to inhibit the 7 major CYP enzymes was investigated using pooled HLM. No inhibition of CYP 1A2, 2B6, 2C8, 2C9, 2C19, 2D6, 3A4/5 was observed after incubation of HBV01 TTRSC02, AAT, givosiran, revusiran, inclisiran, AGT01, AAT02 or HBV02. Weak in vitro inhibition was observed for CYP2B6 and CYP2C8 by cemdisiran. Weak in vitro inhibition was observed for CYP2C8 after incubation with fitusiran and lumasiran.

Figure 2: The potential for a. cemdisiran, b. givosiran, c. HBV01, d. inclisiran and e. fitusiran to induce CYP enzymes through activation of AhR, CAR or PXR was evaluated from 3 separate human hepatocyte donors. No concentration dependent induction of any of the isoforms evaluated was observed. Concentration dependent decreases in mRNA levels for two donors was observed after givosiran treatment.

Figure 3: The potential for a. revusiran, b. fitusiran, c. givosiran and d. inclisiran (single concentration was tested and was set to be much higher than the observed clinical $C_{max,ssu}$ concentration) to act as inhibitors of clinically relevant transporters was investigated. No relevant inhibition was observed for revusiran, fitusiran and inclisiran against any of the transporters evaluated. Givosiran resulted in concentration dependent decreases in P-gp activity.

Figure 4: Correlation analysis of liver enrichment observed in rat versus cynomolgus monkey. In this plot the liver enrichment represents the preferential distribution of GalNAc-siRNAs into liver when compared with plasma (C_{max} liver/C_{max} plasma), since this is a ratio it is unitless.

Tables

Table 1. Clinical PK parameters

GalNAc siRNA	Clinical Dose (mg), clinically relevant unless otherwise noted	Clinical C_{max} (µM)	
		Plasma	Liver projected
revusiran	500	0.058	5.1
HBV01	3 (mg/kg, highest dose tested)	0.057	12
AAT01	6 (mg/kg, highest dose tested)	0.11	29
fitusiran	80	0.0092	4.3
givosiran	2.5 (mg/kg)	0.020	12
inclisiran	300	0.061	17
cemdisiran	600	0.048	12
vutrisiran	25	0.0054	1.9
lumasiran	3 (mg/kg)	0.061	7.1

Table 2. CYP450 reaction phenotyping using rCYP % remaining after designated time-course

Parameter	revusiran	HBV01	AAT01	fitusiran	cemdisiran	vutrisiran	lumasiran
Time point (min)	45	45	45	45	45	45	45
[conc] µM	0.620	0.053	0.614	0.0465	0.0477	0.0490	0.612
CYP1A2	105	97.8	102	106	103	107	103
CYP2B6	104	113	101	103	109	104	100
CYP2C8	98.2	102	103	100	96.1	107	106
CYP2C9	102	87.6	97.5	91.6	101	96.9	99.4
CYP2C19	100	95.8	107	102	102	106	98.8
CYP2D6	98.2	88.8	103	102	110	105	107
CYP3A4	102	108	101	102	95.4	102	94.2
CYP3A5	89.3	97.2	98.6	100	92.9	102	102

Table 3. Time-dependent inhibition results for GalNAc-siRNA against CYPs

CYP isoform	IC_{50} (μM)								
	AAT01			HBV01			givosiran		
	-NADPH	+NADPH	Ratio	-NADPH	+NADPH	Ratio	-NADPH	+NADPH	Ratio
CYP1A2	>614	>614	1	>665	>665	1	>614	>614	1
CYP2B6	>614	>614	1	>665	>665	1	>614	>614	1
CYP2C8	>614	>614	1	>665	>665	1	>614	>614	1
CYP2C9	>614	>614	1	>665	>665	1	>614	>614	1
CYP2C19	>614	>614	1	>665	>665	1	>614	>614	1
CYP2D6	>614	>614	1	>665	>665	1	>614	>614	1
CYP3A4/5 (Midazolam)	>614	>614	1	>665	>665	1	>614	>614	1
CYP3A4/5 (Testosterone)	>614	>614	1	>665	>665	1	>614	>614	1
CYP isoform	IC_{50} (μM)								
	lumasiran			cemdisiran			vutrisiran		
	-NADPH	+NADPH	Ratio	-NADPH	+NADPH	Ratio	-NADPH	+NADPH	Ratio
CYP1A2	>612	>612	1	>596	>596	1	>612	>612	1
CYP2B6	>612	>612	1	>596	>596	1	>612	>612	1
CYP2C8	>612	>612	1	>596	>596	1	>612	>612	1
CYP2C9	>612	>612	1	>596	>596	1	>612	>612	1
CYP2C19	>612	>612	1	>596	>596	1	>612	>612	1
CYP2D6	>612	>612	1	>596	>596	1	>612	>612	1
CYP3A4/5 (Midazolam)	>612	>612	1	>596	>596	1	>612	>612	1
CYP3A4/5 (Testosterone)	>612	>612	1	>596	>596	1	>612	>612	1
CYP isoform	IC_{50} (μM)								
	inclisiran			AGT01			HBV02		
	-NADPH	+NADPH	Ratio	-NADPH	+NADPH	Ratio	-NADPH	+NADPH	Ratio
CYP1A2	>612	>612	1	>18.3	>18.3	1	>20	>20	1
CYP2B6	>612	>612	1	>18.3	>18.3	1	>20	>20	1
CYP2C8	>612	>612	1	>18.3	>18.3	1	>20	>20	1
CYP2C9	>612	>612	1	>18.3	>18.3	1	>20	>20	1
CYP2C19	>612	>612	1	>18.3	>18.3	1	>20	>20	1
CYP2D6	>612	>612	1	>18.3	>18.3	1	>20	>20	1
CYP3A4/5 (Midazolam)	>612	>612	1	>18.3	>18.3	1	>20	>20	1
CYP3A4/5 (Testosterone)	>612	>612	1	>18.3	>18.3	1	>20	>20	1

Table 4. Evaluation of metabolic stability for inclisiran in the incubation media during the induction study

[inclisiran] µM	Donor	% of time = 0 hours (Mean ± SD), n = 3	
		6 hours	24 hours
0.0245	1	99.3 ± 2.09	111 ± 0.76
	2	94.5 ± 1.84	123 ± 2.68
	3	100 ± 1.33	107 ± 4.51
0.245	1	96.1 ± 3.18	117 ± 1.79
	2	98.3 ± 0.83	126 ± 0.29
	3	102 ± 1.31	110 ± 3.92
1.22	1	96.8 ± 2.90	116 ± 6.66
	2	104 ± 1.95	124 ± 7.05
	3	99.3 ± 2.69	114 ± 2.99

Table 5. Confirmation of uptake into sandwich cultured human hepatocytes

GalNAc-siRNA	Nominal incubation concentration (µM)	Measured intracellular concentration (µM) Mean ± SD (n=3)
fitusiran	0.000308	0.0467 ± 0.00761
	0.0154	0.181 ± 0.0315
	0.154	1.12 ± 0.165
	1.54	5.08 ± 1.82
HBV01	0.000665	0.0044 ± 0.000734
	0.00665	0.0271 ± 0.00825
	0.0665	0.687 ± 0.283
	6.65	2.95 ± 1.5
givosiran	0.000613	0.000923 ± 0.0000883
	0.00613	0.0496 ± 0.0081
	0.613	1.34 ± 0.15
	6.13	3.25 ± 1.53
inclisiran	0.0245	0.0571 ± 0.00788
	0.245	0.288 ± 0.038
	1.22	0.734 ± 0.135
cemdisiran	0.0119	0.191 ± 0.027
	0.119	1.04 ± 0.0235
	1.19	3.90 ± 0.368
	11.9	10.1 ± 2.35

Table 6. Assessment of the clinical drug-drug interaction potential based on reversible inhibition of metabolizing enzymes and cutoff criteria from regulatory guidance

GalNAc-siRNA	Enzyme	Ki	Total plasma $C_{max,ss}$ (μM) required to cause clinically relevant inhibition based on DDI guidance criteria [observed clinical concentration at therapeutic dose, μM][a]			R1		Mechanistic static model
			EMA	FDA	PMDA	Plasma	Liver	Liver
cemdisiran	CYP2B6	292	5.83 [0.048]			1.00	1.04	1.03
fitusiran	CYP2C8	28	0.56 [0.0092]			1.00	1.15	1.12
cemdisiran		112	2.24 [0.048]			1.00	1.10	1.08
lumasiran		208	4.16 [0.061]			1.00	1.03	1.03

[a] cutoff = R = 1+50*[I]/Ki, where I is $C_{max,ss,u}$, R $\geqslant$ 2.0 and fu = 1

Figures

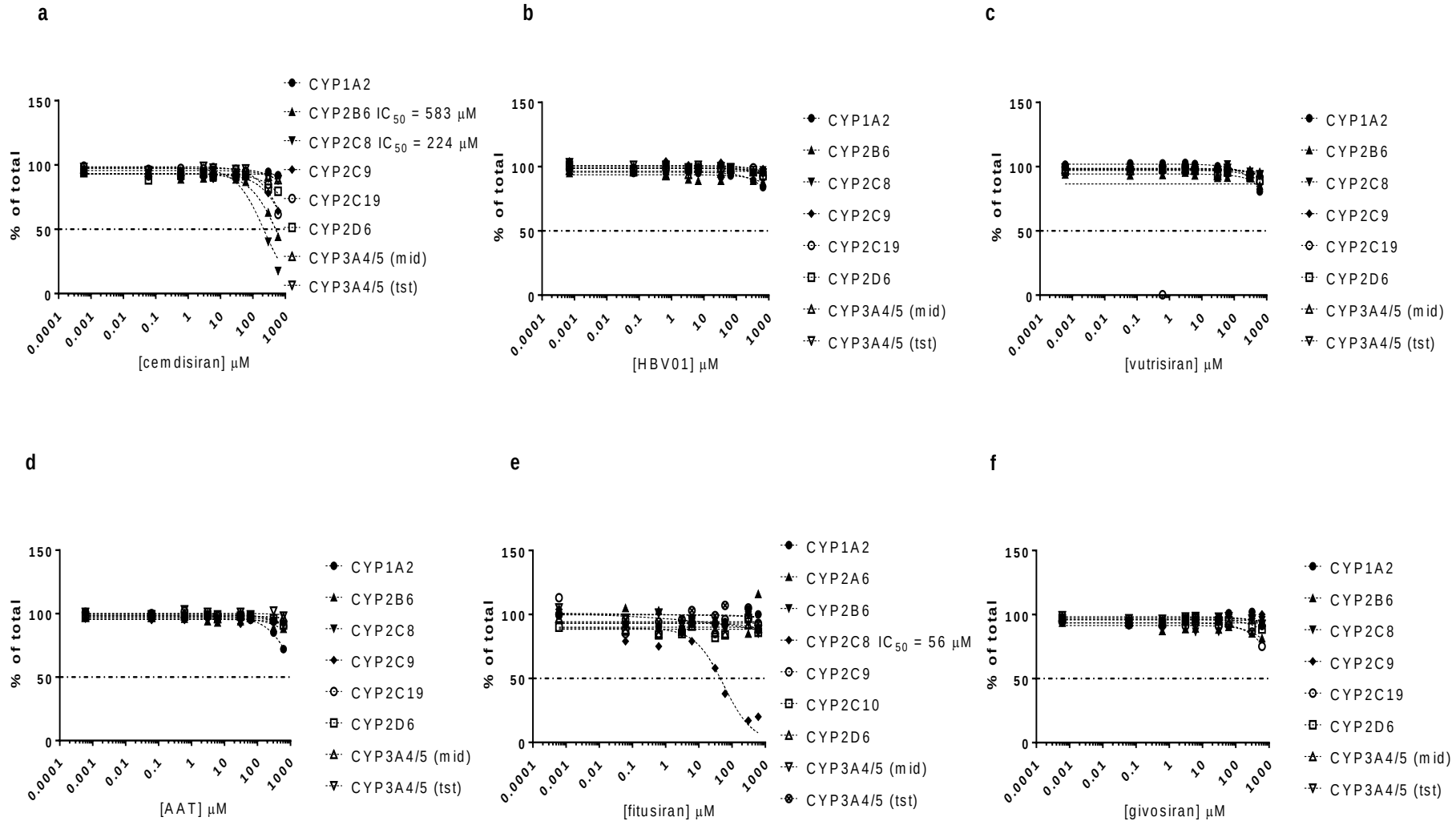

Figure 1

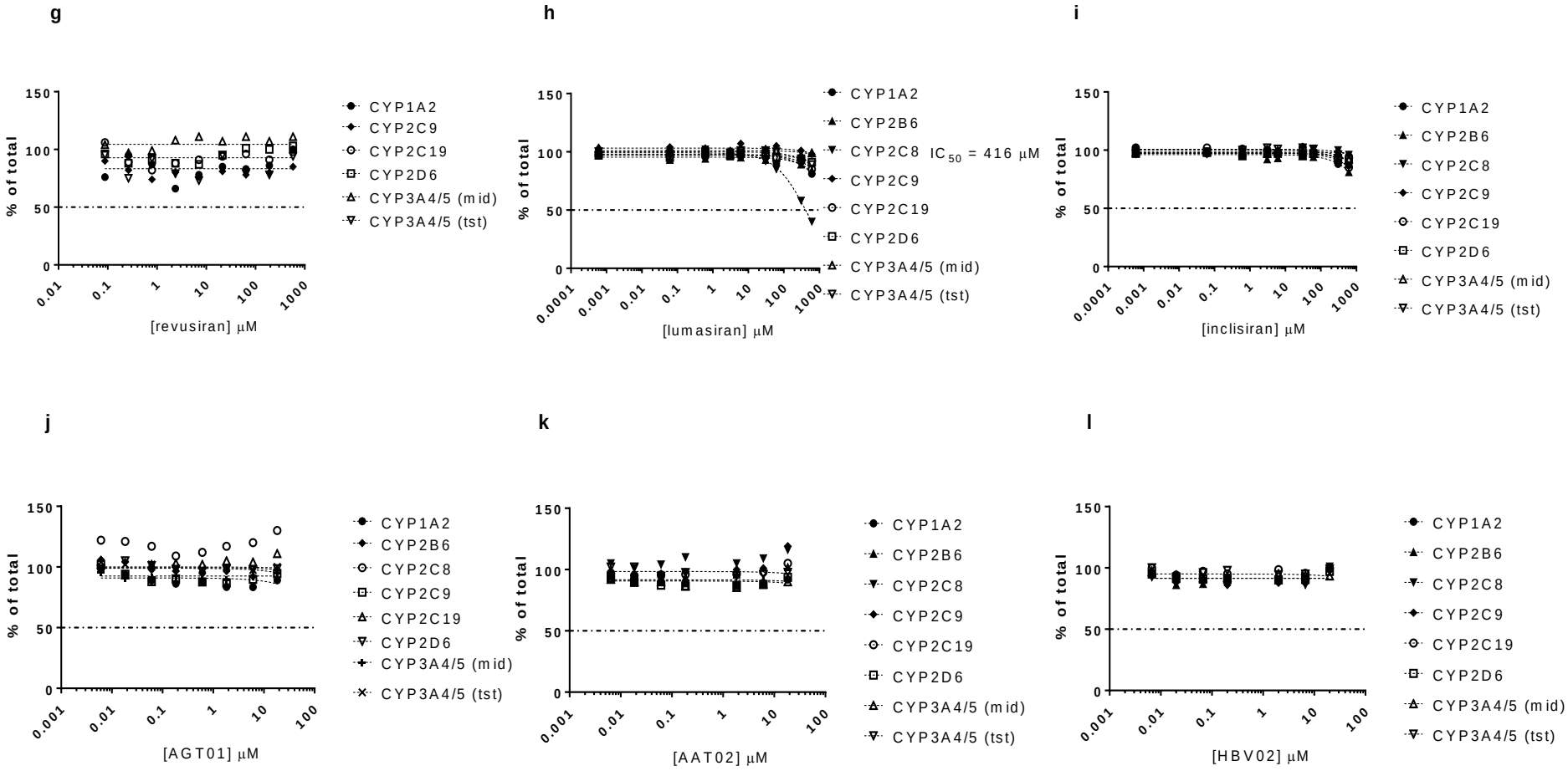

Figure 1 continued

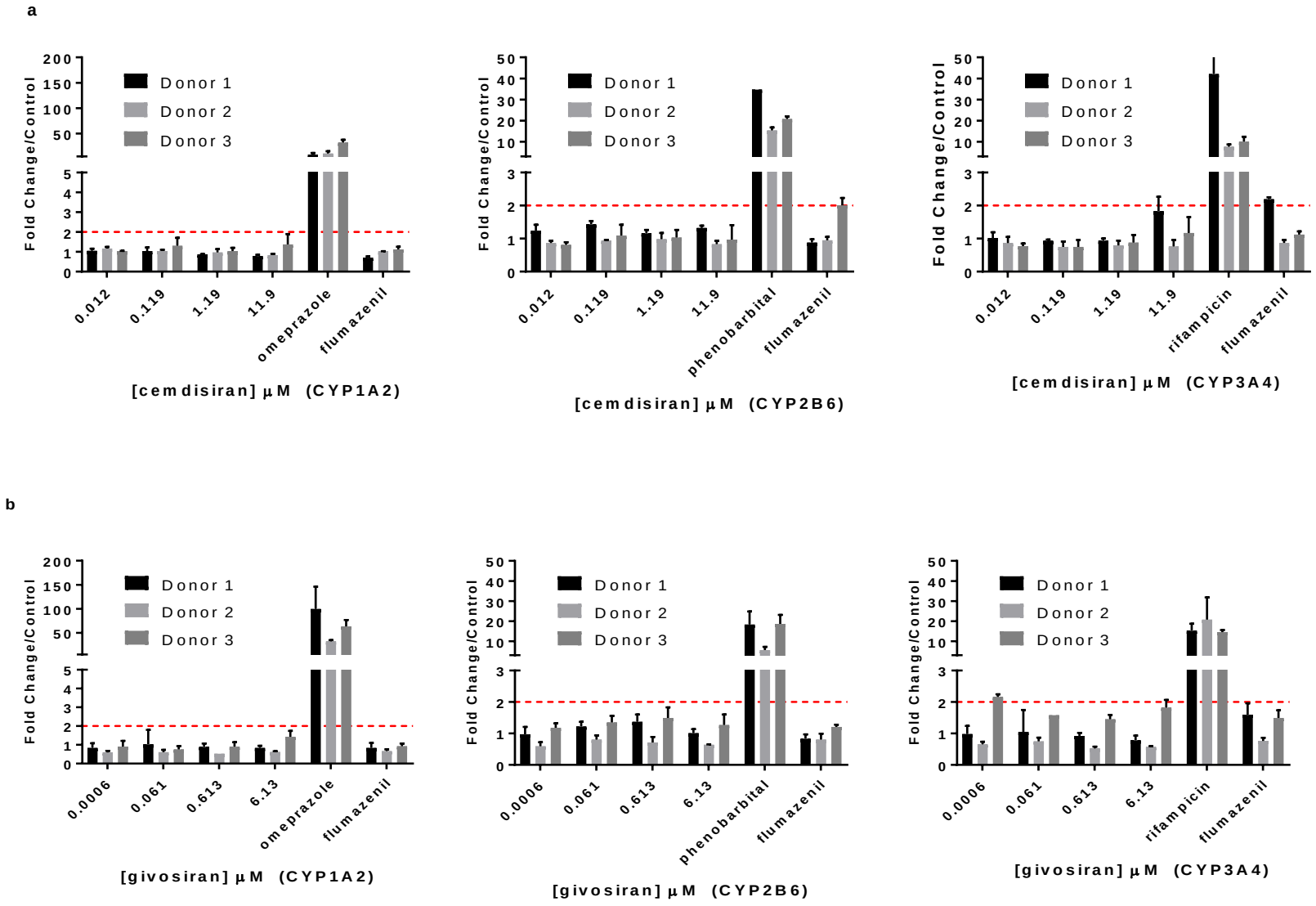
a
Fold Change/Control
Donor 1
Donor 2
Donor 3
0.012
0.119
1.19
11.9
omeprazole
flumazenil
[cemdisiran] µM (CYP1A2)
phenobarbital
[cemdisiran] µM (CYP2B6)
rifampicin
[cemdisiran] µM (CYP3A4)
b
[givosiran] µM (CYP1A2)
0.0006
0.061
0.613
6.13
[givosiran] µM (CYP2B6)
[givosiran] µM (CYP3A4)

Figure 2

c

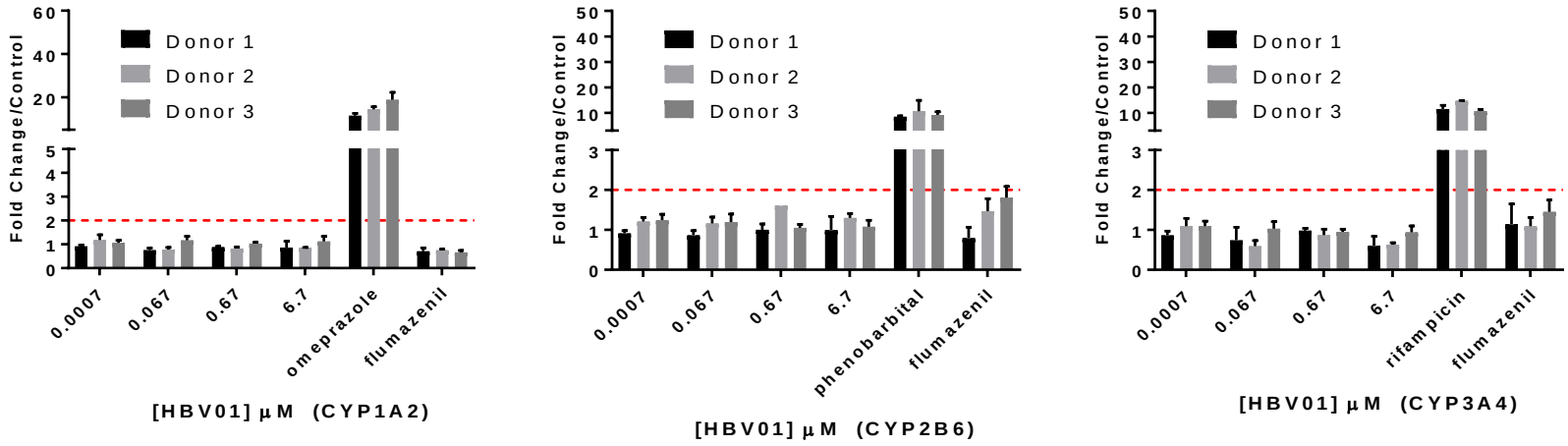

d

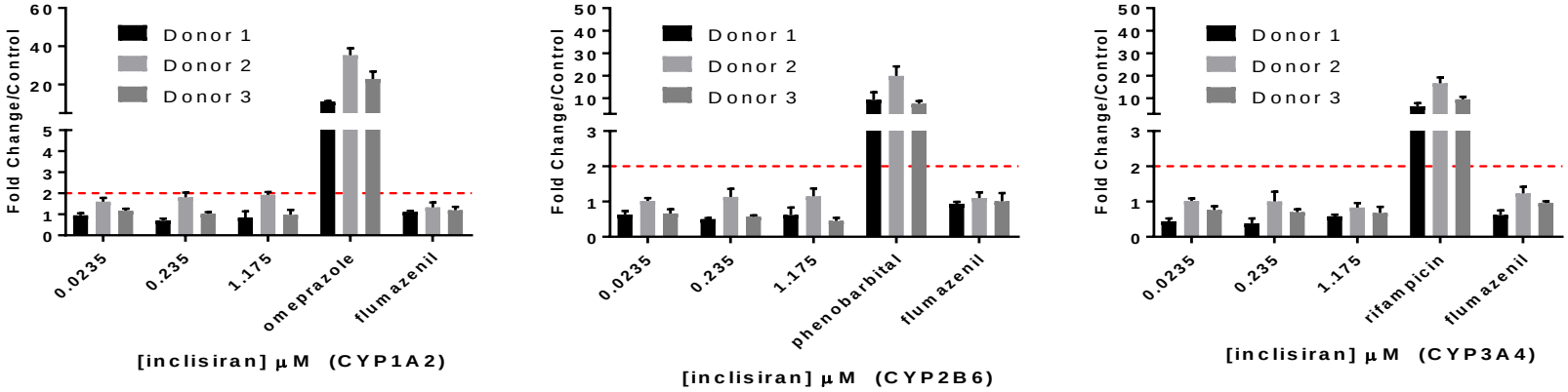

Figure 2 continued

e

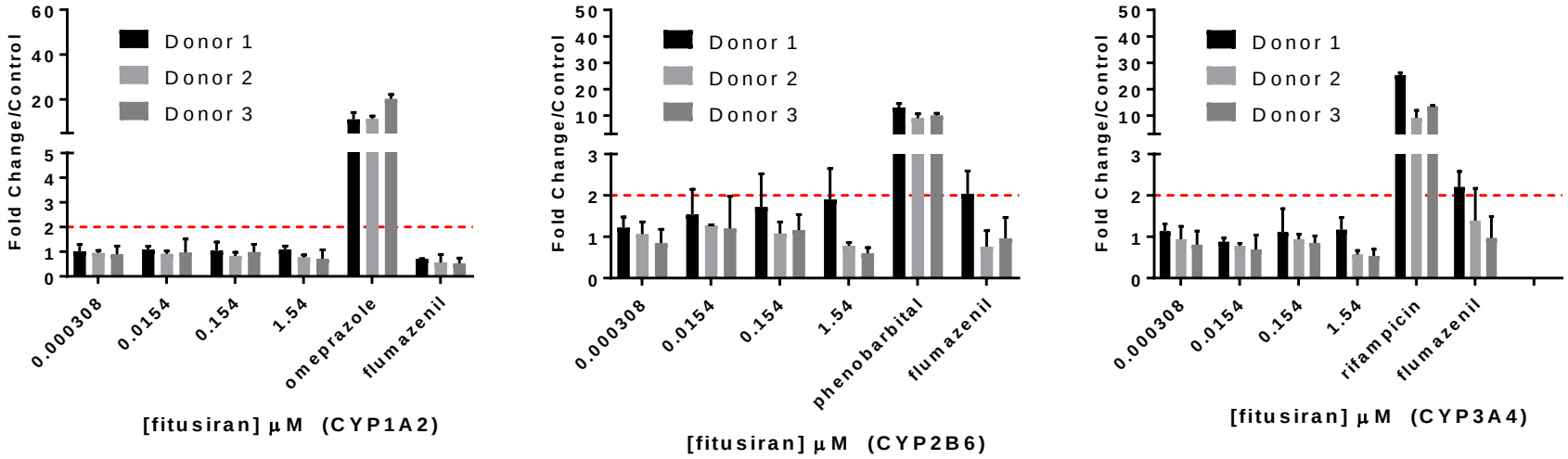

Figure 2 continued

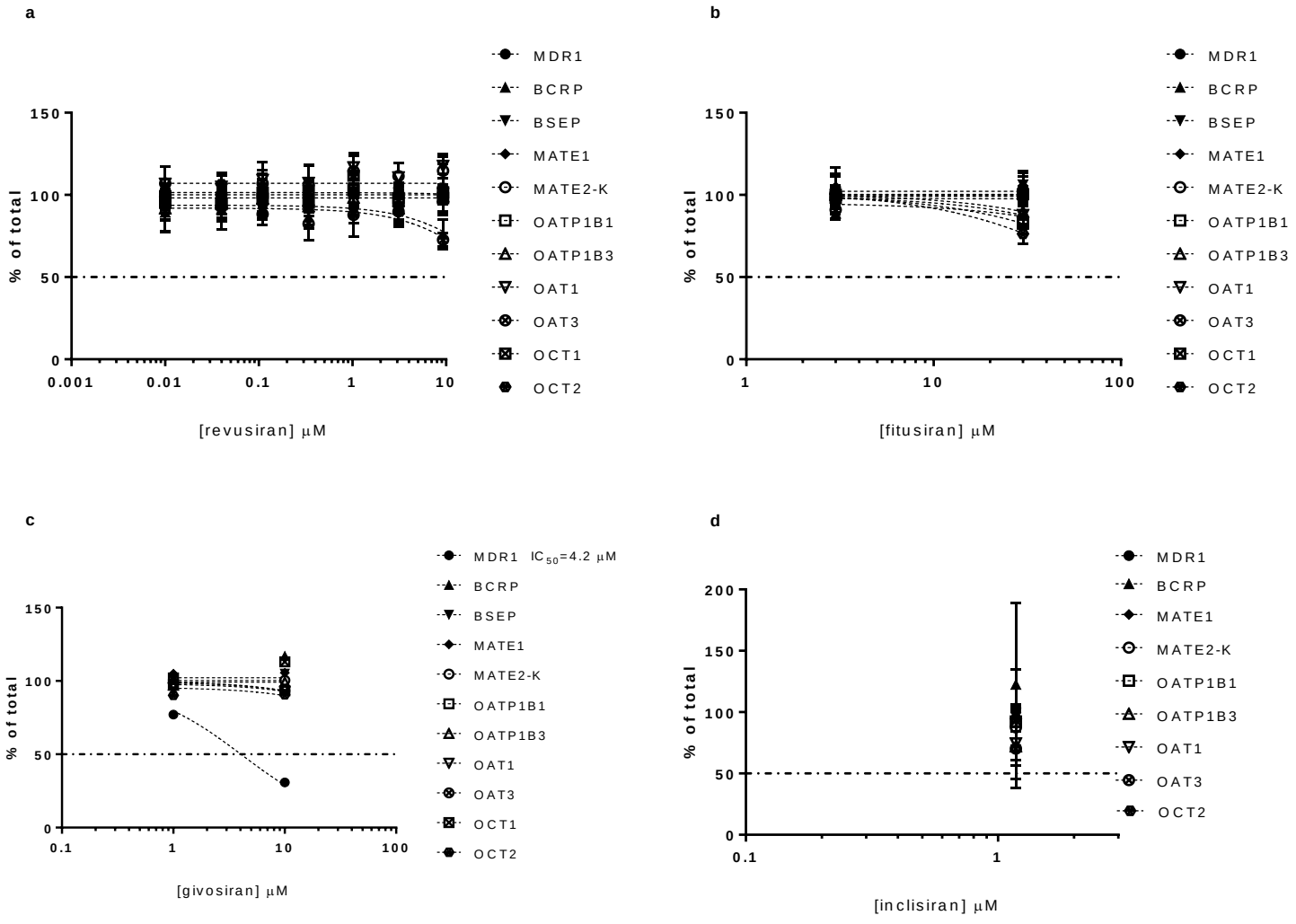
a
% of total
150
100
50
0
0.001
0.01
0.1
1
10
[revusiran] μM
MDR1
BCRP
BSEP
MATE1
MATE2-K
OATP1B1
OATP1B3
OAT1
OAT3
OCT1
OCT2
b
% of total
150
100
50
0
1
10
100
[fitusiran] μM
MDR1
BCRP
BSEP
MATE1
MATE2-K
OATP1B1
OATP1B3
OAT1
OAT3
OCT1
OCT2
c
% of total
150
100
50
0
0.1
1
10
100
[givosiran] μM
MDR1 IC50=4.2 μM
BCRP
BSEP
MATE1
MATE2-K
OATP1B1
OATP1B3
OAT1
OAT3
OCT1
OCT2
d
% of total
200
150
100
50
0
0.1
1
[inclisiran] μM
MDR1
BCRP
MATE1
MATE2-K
OATP1B1
OATP1B3
OAT1
OAT3
OCT2

Figure 3

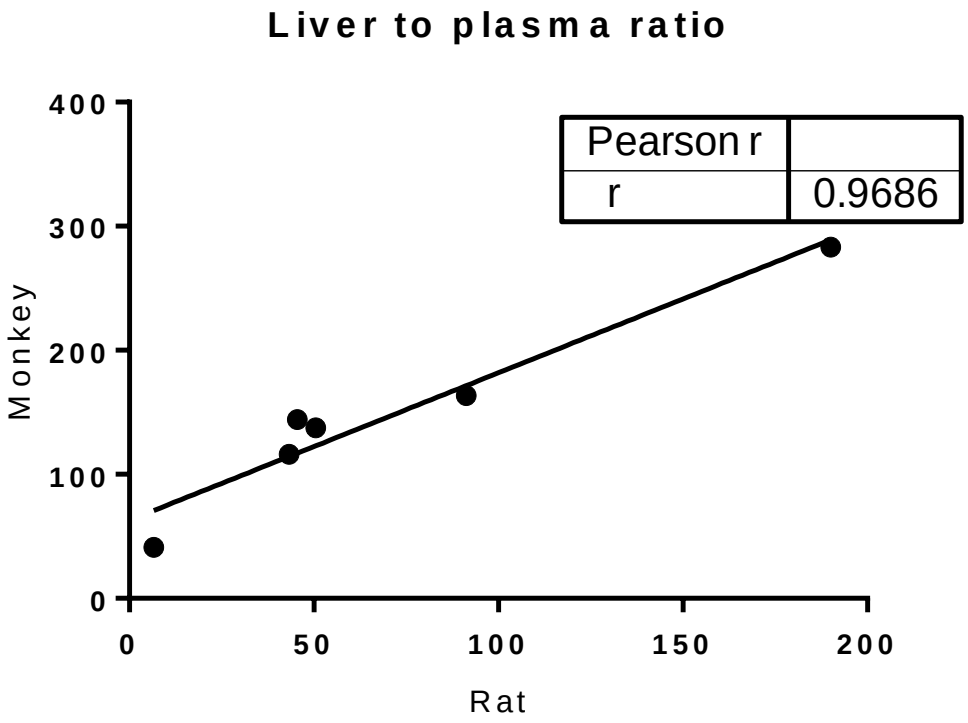
Liver to plasma ratio
Pearson r
r
0.9686
400
300
200
100
0
Monkey
0
50
100
150
200
Rat

Figure 4